Journal of Engineering Science and Technology
Vol. 16, No. 4 (2021) 2950 - 2959

FIBER LASER WELDING OF SIMILAR AND DISSIMILAR ALUMINUM ALLOYS

Y. M. BAQER[1,2,*], S. RAMESH[1,3], F. YUSOF[1], R. MAHMOODIAN[4,5], S. SIVAKUMAR[6], TAO WU[7], CAIWANG TAN[8]

[1]Center of Advanced Manufacturing and Materials Processing, Department of Mechanical Engineering, Faculty of Engineering, University of Malaya, 50603 Kuala Lumpur, Malaysia
[2]Department of Production Engineering and Metallurgy, University of Technology, Baghdad, Iraq
[3]Mechanical Engineering Programme Area, Faculty of Engineering, Universiti Teknologi Brunei, Jalan Tungku Link, Mukim Gadong A, BE1410, Brunei
[4]ULVAC Technologies, Inc. 401 Griffin Brook Dr, Methuen, MA 01844, United States
[5]School of Mechanical Engineering, Universiti Sains Malaysia, 14300, Nibong Tebal, Pulau Pinang, Malaysia
[6]School of Computer Science and Engineering, Taylor's University, No 1, Jalan Taylors, 47500 Subang Jaya, Selangor, Malaysia
[7]School of Mechanics, Civil Engineering and Architecture, Northwestern Polytechnical University, Shaanxi, Xi'an 710072, China
[8]Shandong Provincial Key Laboratory of Special Welding Technology, Harbin Institute of Technology at Weihai, Weihai 264209, China
* Corresponding Author: yaqub.bakir64@yahoo.com

Abstract

Recent studies have emphasized on the deployment of aluminium alloys (AA5083 and AA6061-T6) for automotive industry owing to their excellent corrosion resistance, mechanical properties, and low specific density. Standard welding techniques have been overshadowed by the difficulties associated with joining these alloys. In this research, we investigate the feasibility of fiber laser welding in joining similar and dissimilar AA5083 and AA6061-T6 alloys. The laser power and welding speed were varied to determine the optimum condition to produce a viable welding joint. The properties of the joint such as hardness, and tensile strength were examined. It was found that both macro-voids and solidification cracks occurred in the weldment zone when high welding power (310 W) and high welding speed (24 mm / s.) were used. The presences of micro porosity were inevitable at the optimum welding condition. The study also found that the dissimilar welding of the alloys exhibited improved mechanical properties, this was associated to a refined microstructure and controlled porosity in the weldment.

Keywords: Aluminum alloy, Butt joint, Dissimilar joints, Fiber laser welding.

1. Introduction

Recently, novel manufacturing trends were introduced for lightweight mechanical parts' designs addressing different industrial applications such as automotive industry and electric vehicles manufacturability from car bodies to battery casings which created more opportunities for aluminum alloys utilization [1]. These alloys are becoming more significant in saving cost and energy while reducing environmental pollution. In specific applications or high production processes, it is common to use low-dilution welding rather than fusion welding when joining dissimilar metals.

Because of the high energy, laser welding able to join well dissimilar pieces thus avoiding issues with needing to deal with different thermal conductivities of the base metal. The quest for enhanced performance as well as functionality, hybrid structures comprised of joining two dissimilar metals are needed to take advantage of the properties of both co-joining metals. Non-ferrous materials, such as titanium and aluminum, have been used in industries with the aim of reducing weight and to enhance the performance of components [2]. Aluminum alloys are known for their superior strength, plasticity and corrosion resistance which make them attractive for many applications. The functional specifications of various structural components are met by using dissimilar aluminum alloys, for example in aircraft engines and heat dissipation ducts of electric trains. Improving in the surface texture of a joint can help making it stronger and last longer. Laser beams are viable heat sources for joining aluminum alloys, due to their non-contact and concentrated energy density properties. Nevertheless, defects in the weldment are inevitable such as undercut and crack owing to the differential in the thermal conductivity and expansion coefficients of different aluminum alloys [3].

Laser beam welding allows for a low total heat input to complete a welding while minimizing heat damage to the surrounding base metal. In addition, the weld seam would sustain limited heat affected zone and suffer minimal thermal distortion if compared to conventional welding processes such as metal inert gas (MIG) or tungsten inert gas (TIG). Although, the high optical reflectivity of aluminum alloys may pose a problem during laser welding, ongoing demand for diffusion of high-power Yb: glass fiber lasers operating at 1 μm wavelength has resulted in an improved brilliance at continuous wave power emission thus permitting deep welding to be conducted even having to deal with high reflective metals such as aluminum alloys. In addition, the intense laser beam could overcome the alloy's reflectivity. This in turn is expected to improve the optical absorption and creates the keyhole, allowing the formation of weld seam having high aspect ratio (depth over width), small heat affected zone, higher penetration, and enhanced mechanical properties. Alternatively, the generated keyhole cavity could be affected by weld instability thus causing variety of defects [1]. This keyhole can be defined as a heat source or a primary motor of convection in the melt by producing drag force from the exiting vapor jet [4].

In recent years, laser welding has been developed as new welding technology and has been regarded an appealing heat sources for high speed and deep penetration welding in industrial production and modern intelligent manufacturing processes. The benefit of laser welding over arc welding is that the laser beam can achieve a small spot after being centred by the lens allowing for precise location of the welding position, good quality (narrow and deep weld seams), high processing speed, low cost, low but localized heat input yields, low and predictable distortion

levels, less post-weld reworks, and no mechanical contact between the lance and the work object. It has a long history of use in precision workpiece welding [5, 6].

Casting alloys and wrought alloys are the 2 famous types of aluminum alloys. Some wrought aluminum alloys, such as AA6061-T6, can be heat treated and are widely employed in airplane structure, bicycle body, air coolers, heat pies or exchangers, and heat sink [7], or cold worked, such as (AA5083) alloy, that can be widely utilized in shipbuilding plates, food processing and architectural applications under variety of atmospheric conditions. During the welding, various chemical and physical properties need to be considered while maintaining different joining processes. The welding could also be affected by oxide properties such as hydrogen solubility in molten aluminum as well as thermal, electrical, and nonmagnetic properties which may cause colour change when heated [8, 9]. Both material type and light wavelength or incident radiation can cause the process stability and processing window to increase since the wavelength of the laser decreases [10]. The primary goal of laser welding is to uniformly distribute high energy density on materials which cannot be achieved by simply setting the laser power and speed. Hence, to improve welding accuracy, the focal location of the laser should be controlled by adjusting the laser beam strength along with its welding speed, shielding gas flow rate, the focal distance (i.e., distance between the laser head and the base metal), joint arrangement and beam qualities [11]. The mechanical properties of aluminum welds are extremely sensitive to the above-mentioned laser welding process parameters as reported in the literatures [12-24].

The presented work focused on studying the effect of welding parameters employed for autogenous fiber laser beam welding of AA6061-T6 and AA5083 aluminum alloys with similar and dissimilar materials combination.

2. Methods and Materials

Commercially available aluminum alloys (AA) sheets (2 mm thickness), AA5083 and AA6061-T6 were used in this research. The chemical compositions of the starting base alloys are given in Table 1. The test samples (60×16×2) mm were prepared and the surface was ground in sequence using SiC abrasive sandpapers of grit sizes 400 (rough), 800, and 1200 (fine) grit. The samples were then ultrasonically cleaned in methanol for 6 min. to remove any contaminants and oxide layer on the surface. This was followed by fine polishing using alumina suspension (0.3 μm) and cleaned with ethanol in an ultrasonic bath. The samples were electro-polished using 20 V power source (18113002 EPS 601-China, electrophoresis power supply) for one minute in a solution containing 95% ethanol-5% perchloric acid and prepared for butt welding configuration on one side.

Fiber laser system (Star Fiber Germany, ROFIN-SINAR Technologies Inc., 300) was used in this study. The samples were secured in place as shown in Fig. 1. by using a specially designed jig and fixture to ensure that the laser beam is focussed on the seam of the butt-joint [8]. During the welding, the shielding was accomplished by using argon gas at a flow rate of about 20 l / min.

Table 1. The chemical composition of the starting aluminum alloys.

Elements	Mg	Si	Fe	Cu	Cr	Mn	Zn	Al
AA5083 (wt%)	4.51	0.10	0.21	0.08	0.14	0.62	0.05	Balance
AA6061-T6 (wt%)	1.03	0.71	0.32	0.25	0.25	0.13	0.01	Balance

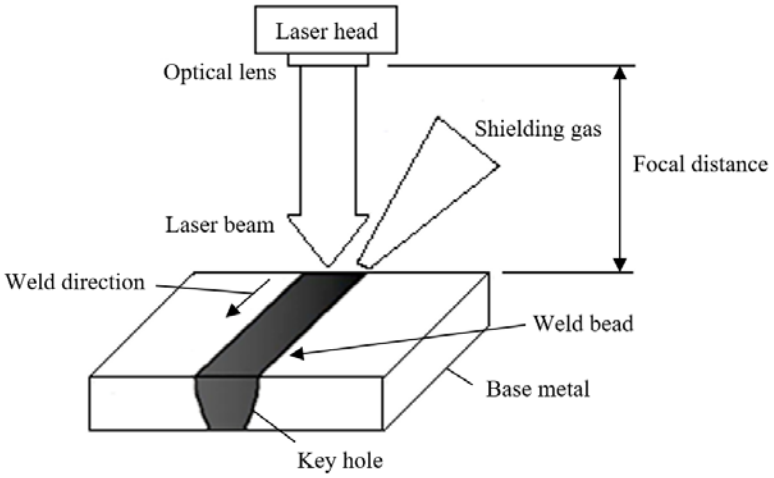

Fig. 1. Schematic diagram of the laser welding process.

The welding parameters selected for this study was selected based on the preliminary study conducted to narrow down the optimum condition to obtain cark free weldment and full depth of penetration. The final welding conditions selected for this work is given in Table 2. In general, the laser power was narrowed down to 270, 290 and 310 W and the welding speed selected was 8, 16 and 24 mm/s. Three different sets of specimen configuration were prepared: similar AA5083 welding, similar AA6061-T6 welding, and AA5083 / AA6061-T6 dissimilar welding. To ensure data reliability, each run was replicated 3 times.

Table 2. Laser welding parameter.

Exp. No.	Laser Power (W)	Welding Speed (mm/s)
1	270	8
2	270	16
3	270	24
4	290	8
5	290	16
6	290	24
7	310	8
8	310	16
9	310	24

For microstructure examination of the welded joint, for similar welded joint, the cut surface was chemically etched in three different solutions: first in Keller's reagent (25% nitric acid + 5% hydrofluoric acid + 70% distilled water) for 5 minutes,

followed by a 3-minute exposure in 10% sodium hydroxide solution and finally in 10% HNO_3 solution for 3 minutes. For dissimilar welded joint, the surface was etched for 3 minutes in 60% hydrochloric acid followed by another 3 minutes in 40% sodium hydroxide solution. In both cases, after each step, the sample was rinsed thoroughly using ethanol and distilled water, and dried. Visual inspections were accomplished by using an optical microscope (Olympus, BX61, 2005, Japan). Energy dispersive spectroscopy (EDX, Zeiss Model-Auriga, 2010, Germany) was used to determine the chemical composition while the phases formed in the welded joint was determined using the X-ray diffraction (XRD-6000, 2009, Shimadzu, Japan).

The Vickers microhardness measurement of the welded section was accomplished using a pyramidal diamond indenter (Model-HV-2 series, 2008, Shimadzu, Japan) with a load of 0.1 kg for 10 s. Hardness measurements were taken at different locations from the centre of the weldment to the base metal with an interval of 0.5 mm.

Tensile test samples were cut from butt joint samples by wire EDM based on the ASTM E8M standard. The geometry and dimensions of the tensile test samples based on the sub-size samples of the standard is shown in Fig. 2. The tensile experiment was conducted using an Instron machine at 10 kN load operating at a 0.5 mm / min. cross head speed. Three samples were tested for each condition and the average value was obtained.

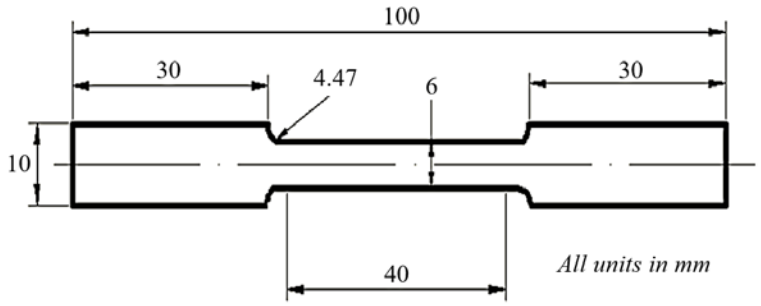

Fig. 2. The geometry and dimensions of the prepared tensile test sample.

3. Results and discussion

The welding experiment found that a complete joint penetration with negligible solidification cracks or undercut was obtained at a moderate welding speed of 16 mm / s. using a laser power of 290 W. This combination of parameters seemed to be the optimum for the aluminum alloys tested in this work. As the power was reduced to 270 W this requires the usage of a low welding speed of 8 mm / s. to achieve an acceptable joint penetration.

In contrast, higher laser power with high welding speed was found to be detrimental as it tends to induce the formation of solidification cracks as well as large pore-like voids in the weldments especially for the similar AA6061-T6 joint as typically shown in Fig. 3. Hence, for subsequent test, the welding was conducted using a laser power of 290 W at a welding speed of 16 mm / s. to ensure a fair comparison could be made across the three joints.

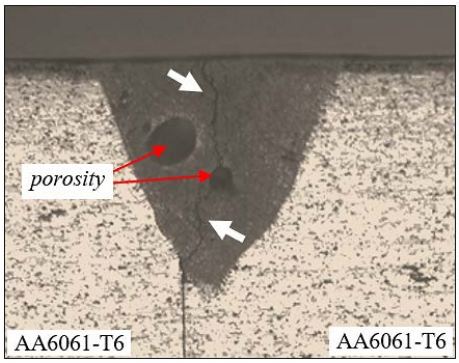

Fig. 3. Solidification cracks (white arrows) observed in the weldment of similar AA6061-T6 joint made using 310 W and 24 mm / s.

In general, a smooth and uniform weld beads were observed via visual inspection for all joints when the welding was performed at 290 W and 16 mm / s. as shown in Fig. 4. A uniform weldment was observed however the cross-section of the keyholes showed the presences of some porosities at the fusion zone. A general observation is that the microstructure of the welded joints was refined when compared to the base metal. This could be associated to the fast cooling resulting from laser beam scanning [9]. Figure 4. also indicated that the similar AA6061-T6 and dissimilar joints exhibited larger pores than the similar 5083 joints. This porosity could be associated with melting and evaporation of the metal at the fusion zone [25, 26].

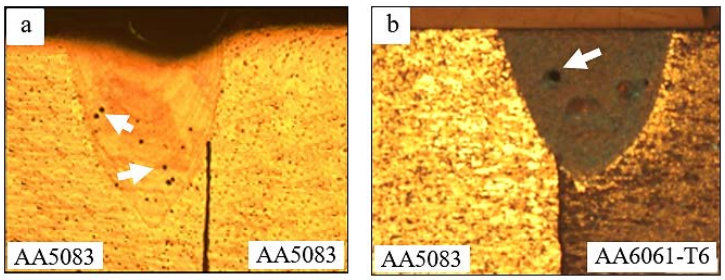

Fig. 4. Optical micrographs of keyholes produced from:
(a) Similar AA5083 joint and
(b) Dissimilar AA5083 / 6061-T6 joint.
The pores are as shown by the arrows in the figures.

According to the literatures that when the welded beads' magnesium content is more than 2%, which was expected for the dissimilar joints in the present work, the liquid quickly oxidizes to form magnesium oxide (MgO) and aluminum magnesium (Al_3Mg_2) [24] as well as the rate of hydrogen porosity increased rapidly. This occurs because magnesium in aluminum alloys improves the molten pool's hydrogen solubility. Hydrogen porosities can be decreased by using higher welding speeds which limits the growth of the hydrogen porosities. For 3 alloys (2 similar and 1 dissimilar), it was clear that the interaction of ambient hydrogen with ambient oxygen during the welding process has a significant influence on the porosity in the weld seam. Furthermore, it cannot be ruled out that the presence of

water vapor in liquid aluminum could also cause some pore formation due to water molecule dissociation during the welding process [26].

When welding at moderate laser power (290 W) and high speed (24 mm / s.) with continuous wave, the heat affected zone is small. In addition, a higher welding speed could reduce the porosity, but spatter would be created along the keyhole boundaries because of the instability of the weld pool [22, 23]. The XRD analysis of the welded joints revealed a mix phase formation at the weldment with Al_2O_3 as major and Al_2MgO_4, MgO and $Fe_2Si_2Al_9$ being the minor phases.

The combine effect of welding speed and laser power on the tensile strength of the welded joints is shown in Fig. 5. The results indicated that for all test conditions the highest tensile strength was exhibited by the dissimilar welded samples. The detail test results are presented in Table 3. It was found that the dissimilar joining of the aluminum alloy yielded improved properties if compared to the similar welded joints.

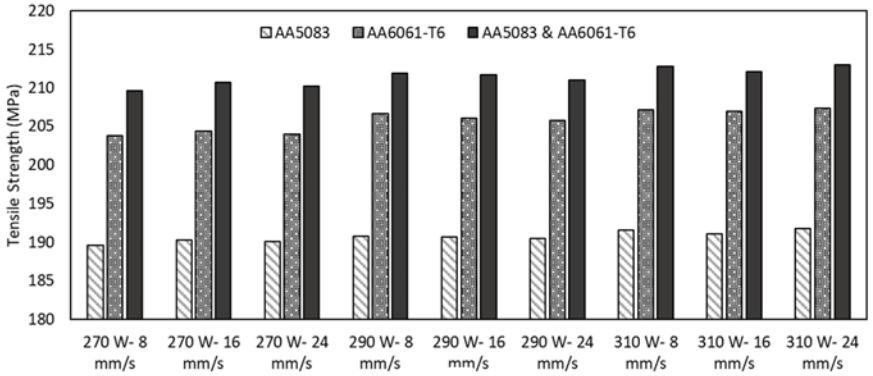

Fig. 5. The effect of welding parameter on the tensile strength of similar and dissimilar welded samples.

Table 3. Tensile properties of the welded joints.

Properties	Similar Welding AA5083	Similar Welding AA6061-T6	Dissimilar Welding AA5083 / AA6061-T6
Tensile Stress at break (standard) (MPa)	104.7	96.2	161.9
Tensile strain at break (standard) (%)	5.04	4.86	5.45
Yield Stress (slope @ 0.002%) (MPa)	156.00	157.37	193.19
Maximum Tensile Stress (MPa)	191.85	207.32	213.05
Elastic Modulus (GPa)	79	78.1	85.2

The Vickers microhardness variation for the dissimilar welded joint is shown in Fig. 6. The AA5083 base metal (BM) exhibited a low hardness of about 53 ± 3 HV whereas the AA6061-T6 recorded a higher value of 73 ± 2 HV. A general trend observed was that the hardness improved over the weldment of the dissimilar joint

when compared to the AA5083 base metal. A higher hardness was measured in the heat affected zone (HAZ) at the AA6601-T6 side.

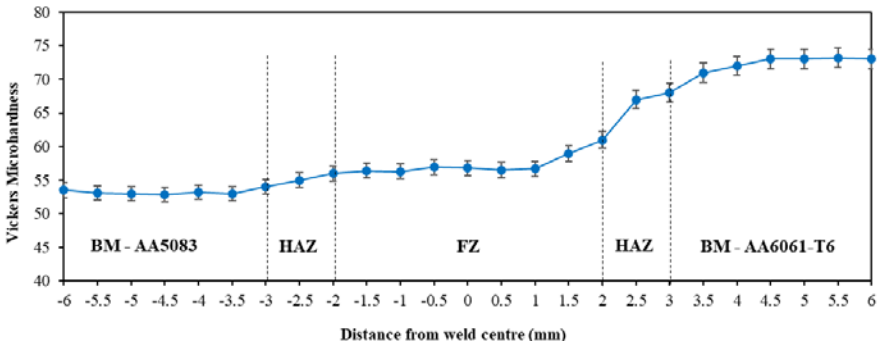

Fig. 6. Vickers microhardness (HV) profile through the weldment for dissimilar AA5083 / AA6061-T6 alloy welded joint.

Conclusions

In this study, fiber laser welding was used to join AA5083 and AA6061-T6 aluminum sheets using varying laser power and welding speed. The weldment microstructural and mechanical properties were evaluated, and the laser power and welding speed was found to have an impact on the properties of the joints. Welding at 290 W and welding speed of 16 mm / s. were found to be optimum to obtain a sound weldment, having controlled porosity. In all joints, the welding beads' micro porosity and pore defects increased as welding speed was increased. Enhancement of mechanical properties was observed for the dissimilar aluminium joint, this was attributed to the refined microstructure of the weldment and the absent of solidification cracks.

Nomenclatures

AA	Aluminum alloy
Al_2O_3	Aluminum oxide
BM	Base metal
FZ	Fusion zone
HV	Vickers hardness
HAZ	Heat affected zone
MgO	Magnesium oxide
XRD	X-ray diffraction

References

1. Garavaglia, M.; Demir, A.G.; Zarini, S.; Victor, B.M.; and Previtali, B. (2020). Fiber laser welding of AA 5754 in the double lap-joint configuration: process development, mechanical characterization, and monitoring. *The International Journal of Advanced Manufacturing Technology*, 111, 1643-1657.
2. Janasekaran, S.; Lemon, S.M.B.; and Yusof, F. (2019). Influence of welding parameters on lap joint between Al and Ti alloys using low power fiber laser. *Materialwissenschaft und Werkstofftechnik*, 50(3), 346-352.

3. Chen, C.; Xiang, Y.; and Gao, M. (2020). Weld formation mechanism of fiber laser oscillating welding of dissimilar aluminum alloys. *Journal of Manufacturing Processes*, 60, 180-187.
4. Kumar, M.R.; Jouvard, J.M.; Tomashchuk, I.; and Sallamand, P. (2020). Vapor plume and melted zone behavior during dissimilar laser welding of titanium to aluminum alloy. *Proceedings of the Institution of Mechanical Engineers, Part L: Journal of Materials: Design and Applications*, 234(5), 681-696.
5. Tang, X.; Zhong, P.; Zhang, L.; Gu, J.; Liu, Z.; Gao, Y.; Hu, H.; and Yang, X. (2020). A new method to assess fiber laser welding quality of stainless steel 304 based on machine vision and hidden Markov models. *IEEE Access*, 8, 130633-130646.
6. Ramakrishnan, V.S.M.; and Gautam, J.P. (2020). Optimization of post weld heat treatment cycle of fiber laser welded bainitic steel. *E3S Web of Conferences*, 184: Article Number 01039.
7. Harvey, J.P.; and Chartrand, P. (2010). Modeling the hydrogen solubility in liquid aluminum alloys. *Metallurgical and Materials Transactions B*, 41, 908-924.
8. Lin, R.Y.; and Hoch, M. (1989). The solubility of hydrogen in molten aluminum alloy. *Metallurgical Transactions A*, 20A, 1785-1791.
9. Xiao, R.; and Zhang, X. (2014). Problems and issues in laser beam welding of aluminum–lithium alloys. *Journal of Manufacturing Processes*, 16(2), 166-175.
10. Fortunato, A.; and Ascari, A. (2019). Laser welding of thin copper and aluminum sheets: feasibility and challenges in continuous-wave welding of dissimilar metals. *Lasers in Manufacturing and Materials Processing*, 6, 136-157.
11. Stavridis, J.; Papacharalampopoulos, A.; and Stavropoulos, P. (2018). Quality assessment in laser welding: A critical review. *The International Journal of Advanced Manufacturing Technology*, 94, 1825-1847.
12. Miyagi, M.; Wang, H.; Yoshida, R.; Kawahito, Y.; Kawakami, H.; and Shoubu, T. (2018). Effect of alloy element on weld pool dynamics in laser welding of aluminum alloys. *Scientific Reports*, 8, Article number: 12944.
13. Lu, Q.; Yu, Z.; Zhang, P.; Yan, H.; and Li, C. (2019). Laser welding process evaluation on stake-welded T-joints. *Materials Research Express*, 6, 0865a4.
14. Zhao, H.; and Debroy, T. (2001). Weld metal composition change during conduction mode laser welding of aluminum alloy 5182. *Metallurgical and Materials Transactions B*, 32, 163-172.
15. Dharmendra, C.; Rao, K. P.; Wilden, J.; and Reich, S. (2011). Study on laser welding–brazing of zinc coated steel to aluminum alloy with a zinc based filler. *Materials Science and Engineering A*, 528(3), 1497-1503.
16. Cao, X.; Wallace, W.; Immarigeon, J.P.; and Poon, C. (2003). Research and progress in laser welding of wrought aluminum alloys. II. Metallurgical microstructures, defects, and mechanical properties. *Materials and Manufacturing Processes*, 18(1), 23-49.
17. El-Batahgy, A.; and Kutsuna, M. (2009). Laser beam welding of AA5052, AA5083, and AA6061 aluminum alloys. *Advances in Materials Science and Engineering*, Volume 2009, Article ID 974182.
18. Chua, S.F.; Chen, H.C.; and Bi, G. (2019). Influence of pulse energy density in micro laser weld of crack sensitive Al alloy sheets. *Journal of*

Manufacturing Processes, 38, 1-8.

19. Çevik, B.; and Gülenç, B. (2018). The effect of welding speed on mechanical and microstructural properties of 5754 Al ($AlMg_3$) alloy joined by laser welding. *Materials Research Express*, 5, 086520 .
20. Katayama, S.; Nagayama, H.; Mizutani, M.; and Kawahito, Y. (2013). Fibre laser welding of aluminium alloy. *Welding International*, 23(10), 744-752.
21. Tu, J.F.; and Paleocrassas, A.G. (2010). *Laser welding*. Chapter: Low speed laser welding of aluminium alloys using single-mode fiber lasers. InTechOpen, 46-76.
22. Wu, D.; Hua, X.; Li, F.; and Huang, L. (2017). Understanding of spatter formation in fiber laser welding of 5083 aluminum alloy. *International Journal of Heat and Mass Transfer*, 113, 730-740.
23. Cao, X.; Wallace, W.; Poon, C.; and Immarigeon, J.P. (2003). Research and progress in laser welding of wrought aluminum alloys. I. Laser welding processes. *Materials and Manufacturing Processes*, 18(1), 1-22.
24. Highway, A.A.S.; and Officials, T. (2004). Materials, E8M-04 Standard test methods for tension testing of metallic materials (Metric) 1. ASTM Int.
25. Alter, L.; Heider, A.; and Bergmann, J.P. (2020). Influence of hydrogen, oxygen, nitrogen, and water vapor on the formation of pores at welding of copper using laser light at 515 nm wavelength. *Journal of Laser Applications*, 32, 022020 .
26. Li, J.; Cai, Y.; Yan, F.; Wang, C.; Zhu, Z.; and Hu, C. (2020). Porosity and liquation cracking of dissimilar Nd: YAG laser welding of SUS304 stainless steel to T2 copper. *Optics and Laser Technology*, 122, 105881.